Kinetics of crystallization in a shearing colloidal suspension

Scott Butler and Peter Harrowell
Department of Physical and Theoretical Chemistry, University of Sydney, Sydney, New South Wales 2006, Australia
(Received 11 July 1995)

We report the kinetics of crystallization as observed in simulations of a charged colloidal suspension under shear. We find that the imposed shear flow inhibits crystal nucleation. Crystallization was only observed for shear rates at or below $\dot{\gamma}\tau_0=0.07$ (where τ_0 is the time required for a particle to diffuse the averge interparticle distance in a dilute suspension). Under the influence of these low shear rates the suspension crystallizes into a single shear-aligned crystal, as opposed to the polycrystalline structure found in the absence of shear flow. Crystal growth is found to be proportional to the effective supercooling, as measured from the melting temperature of the shearing crystal. We conclude that, by analogy with the case of crystallization at zero shear, the effective supercooling provides an operational measure of the "thermodynamic" stability of the shearing crystal.

PACS number(s): 64.70.Dv, 62.20.−x, 82.70.Dd

I. INTRODUCTION

In this paper we describe the kinetics of crystallization as observed in simulations of amorphous charged colloidal suspensions undergoing shear flow. That such a process occurs in reality is indicated by experimental reports [1] of the development of long-range periodic order in shearing suspensions as the shear rate is lowered. However, we are unaware of any quantitative studies, either experimental or using computer simulation, of the kinetics of this ordering process in flowing liquids. In the following section we shall consider some of the basic physical questions raised by crystallization under shear. Some of these expectations are compared with the effects of the applied shear on nucleation from the melt, as well as the propagation of a planar crystal surface observed in the simulated suspension.

II. THEORY

To begin, we shall need to introduce two general observations concerning the effects of an applied shear on the stability of crystalline order in a suspension. The first is that a crystal can sustain a substantial amount of its three-dimensional structure while being forced to slowly shear *only if* the shear gradient is normal to a particular crystal plane (typically the closest-packed plane) and the flow is aligned along a close-packed direction in this plane. In the case of a body-centered cubic (bcc) structure, the appropriate plane is the (110) and the selected direction in this plane is [111]. This is the only orientation that has been observed in light scattering studies [1] of charged polystyrene colloids, which, at low concentrations of added salt, form stable bcc crystals. For the face-centered cubic (fcc) crystal [2] the sliding planes are observed to be the (111) planes which move in the [111] direction. In simulations we can alter the crystal orientation with respect to the shear flow in order to see what will happen. The result is rapid disordering at the lowest shear rates studied [3–6] at all orientations chosen other than the unique "easy" direction.

The second observation is that colloidal crystals, even when properly aligned with the shear flow, will undergo a disordering transition to the amorphous suspension as the shear rate is increased beyond a critical value. This is the case, for example, in the low salt suspension of polystyrene particles studied by Ackerson and Clark [1]. This disordering transition has also been observed in nonequilibrium simulations [5,6]. The physical origins of this shear-induced disordering transition have yet to be established. Recently, [6] we suggested a mechanism involving the shear-induced generation of interstitial defects, which leads to the destabilization of long-range order via a collective process similar to defect-induced amorphization. One of the motives for this present study is to explore the possibility that the kinetics of crystallization provides a useful way of quantifying the relative stability of the crystalline and amorphous steady states in the shearing suspension.

Now we can consider the nucleation of a sliding crystal from the shearing suspension. We assume that the structural fluctuations in the suspension can be represented as a distribution of crystallites of different sizes. At zero shear this distribution is determined by the metastable equilibrium of the supercooled liquid and by the critical nucleus size above which the cluster is unstable to growth. In the steadily shearing suspension, the fate of a crystallite will be influenced by the shear flow in at least three ways. (i) A crystallite that is not "correctly" oriented with the shear as described above will not be able to shear *and* retain crystalline order. These clusters will either be sheared, and hence destroyed, or they will resist shear and rotate until they are "correctly" aligned, at which point they will shear with the possibility of retaining some crystalline order. (ii) A shearing crystallite will be destroyed if the shear rate convects layers past one another faster than the layers can grow. (iii) The nucleation rate is expected to be a sensitive function of the difference in stability of the shearing crystal structure to that of the shearing liquid. This difference will depend on

the shear rate.

Which of the two outcomes described in process (i) actually occurs will depend on the rotational friction experienced by a cluster. The larger the resistance to rotation, the greater will be the internal stress in the cluster due to the applied shear. Because it is true that the smaller the cluster, the lower the rotational friction, we shall assume that all clusters in a liquid have an ancestor small enough to have been rotated and aligned by the shear. The result of this is that at the point at which crystalline fluctuations are of a critical size, they are assumed to be aligned with the shear. That is, we expect that the rate of nucleation will not be diminished compared to the rate at zero shear because of the destruction of crystallites of "incorrect" orientation.

A decrease in the nucleation rate *would* be expected from the process labeled (iii). To force crystal layers to slide over one another is to perturb the equilibrium configuration. To the extent that equilibrium concepts retain relevance with regard to crystalline stability in the shearing liquid, this perturbation would be expected to destabilize the crystal with respect to the liquid. Let us represent this as a decrease of the *effective* supercooling ΔT_{eff}. We can define ΔT_{eff} operationally as the difference at a given shear rate $\dot{\gamma}$ between the actual temperature and the transition temperature of the shear-induced disordering. It immediately follows from this definition that for those systems that do not exhibit shear-induced disordering, $\Delta T_{\text{eff}}=\Delta T$. At small shear rates we might hope to approximate the effective supercooling by

$$\Delta T_{\text{eff}} \approx \Delta T - \mu\dot{\gamma} \ . \tag{1}$$

(Please note that this simple expression is being used for the purpose of discussing the crystallization rates only. We have argued elsewhere [6] that the effect of an applied shear on crystalline stability is considerably more complex than such pseudoequilibrium descriptions imply. The shear-induced disordering transition involves a range of intermediate structures that have no analog in the equilibrium melting transition.) If we were to indicate on the T-$\dot{\gamma}$ plane a "nucleation" line below which homogeneous crystal nucleation achieves an observable rate, then the perturbation expressed in Eq. (1) would appear as indicated in Fig. 1.

The critical nucleus is identified as the smallest cluster that is unstable with respect to growth to a bulk crystal. In the shearing liquid one more obstacle stands in the way of such a cluster growing to bulk size. If the planes of a finite sized cluster are shearing past one another, eventually they will be convected on into the surrounding liquid and the cluster destroyed [process (ii)] unless the crystal growth rate matches or exceeds the convection rate. This leads us to define a critical shear rate $\dot{\gamma}_{\text{crit}}$, in terms of the crystal growth rate v and a, the interlayer spacing, as

$$\dot{\gamma}_{\text{crit}} = v/a \ . \tag{2}$$

Only for shear rates $\dot{\gamma} \leq \dot{\gamma}_{\text{crit}}$ will growth win over convective disordering. While not a major consideration, it is interesting to note that the appropriate growth rate to use in Eq. (2) is that of a high index surface. Growth along the line of flow will always occur at a surface with high step density, thanks to the convection of layers (see Fig. 2). The crystal growth rate v would be expected to be proportional to the effective supercooling, so that

$$\dot{\gamma}_{\text{crit}} = c\Delta T_{\text{eff}}/a \ , \tag{3}$$

with c a constant. This line is also sketched in Fig. 1 [using the linear expression for ΔT_{eff} in Eq. (1)].

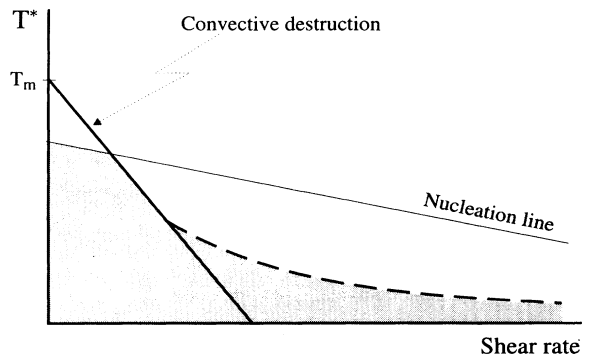

FIG. 1. Schematic representation of nucleation behavior under variations in temperature and shear rate. The "nucleation line" shows the expected decrease in nucleation due to destabilization of the equilibrium structure by the applied shear. This line is cut by the line representing the effect of "convective destruction" of nuclei. At low temperatures, where nucleation occurs at many sites, a nonlinearity is expected in the convective destruction of nuclei. This is represented by the dashed line. The shaded area is therefore the window of temperatures and shear rates within which nucleation and growth of order are expected to occur.

The condition specified in Eq. (3) may well be too restrictive. It establishes the relationship between shear rate and growth rate such that the former will never outstrip the latter for arbitrary periods of time. In reality, however, a crystallite only needs to grow far enough to meet neighboring crystallites. As the distance between neighboring clusters is a rapidly decreasing function of supercooling, we would expect the critical shear curve in Fig. 1 to exhibit a nonlinear dependence, as indicated qualitatively by the dashed line. The increased window for observable nucleation that this modification affords arises from the possibility of sliding layers of neighboring clusters overlapping with one another and so avoiding the de-

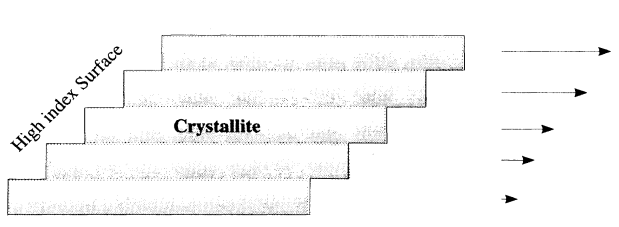

FIG. 2. Schematic diagram showing a crystallite undergoing plane-over-plane sliding under shear. The result of layers sliding over one another is the production of stepped high index surfaces from which growth must occur if the cluster is not to be destroyed by convection.

struction experienced by an isolated crystallite. Note that together, the nucleation line and the critical shear line restrict the region in which crystal nucleation would be observable. Within this window we would expect to see the nucleation rate decrease with increasing shear rate as a result of the decreasing effective supercooling.

This "window" of observable nucleation would be expected to differ from that shown in Fig. 1 in the case of oscillatory flows. We have not carried out simulation studies of the crystallization kinetics in such flows and so shall consider them only briefly here. Let us characterize an oscillatory shear flow by a shear rate and an amplitude of oscillation so that as the amplitude goes to infinity, the flow becomes a steady shear. As long as the amplitude is greater than the particle spacing, process (i) would be the same as for the steady flow. For amplitudes of oscillation smaller than the size of a crystal cluster, however, we would expect the convective destruction described in process (ii) to be significantly reduced. Small amplitude oscillations would not convect crystal layers far enough from their neighbors to result in complete disordering. In fact, such motion may enhance growth of a larger-than-critical cluster by generating high index surfaces (as depicted in Fig. 2). Both experimental [7] and simulation [8] studies indicate that layered structures can be stabilized in suspensions by oscillatory shears. It is possible that, for small enough oscillatory amplitudes, the applied shear may be regarded as stabilizing crystalline order rather than causing the destabilization described for steady shears in process (iii).

Turning now to the growth of a planar interface in the presence of a steady flow, processes (i) and (ii) become irrelevant (as long as we are not interested in the case in which the shear flow is directed normal to the interface). We would expect that result already proposed above for the dependence of the growth rate on the applied shear rate, i.e.,

$$v = c\Delta T_{\text{eff}} . \tag{4}$$

At this simple level of theory we propose to make no distinction between the case in which the shear gradient is normal to the surface and the one in which it lies in the plane of the surface.

III. DETAILS OF THE BROWNIAN DYNAMICS SIMULATIONS

We would like to compare the result for a simulated shearing colloidal suspension with the predictions described above. We chose to model charged colloidal particles suspended in aqueous salt solution. The ability to change the range of particle interactions simply by changing the salt concentration in the solvent has made these systems amenable to experiment. Such systems have been shown to form bcc, fcc, and amorphous structures at rest [9] and, as mentioned earlier, can sustain order over a range of shear rates [1].

The algorithm we used to model the dynamics of colloidal particles under shear was the Brownian dynamics algorithm of Ermak [10], with the addition of a shearing term. We define the shear velocity to be in the x direction, the shear gradient in the y direction, and the vorticity in the z direction. The resulting nonequilibrium Brownian dynamics algorithm for particle propagation in overdampled conditions in the presence of a linear velocity field is

$$\Delta \mathbf{r}_i = (\dot{\gamma} y_i \mathbf{e}_x + D_0 \mathbf{F}_i / k_b T)\Delta t + \mathbf{R}_i , \tag{5}$$

where $\Delta \mathbf{r}_i$ is the change per time step in the position vector of particle i, D_0 is the free diffusion constant, Δt is the time step, $\dot{\gamma}$ is the applied shear rate, y_i is the position of particle i along the shear gradient, $\mathbf{e}_x$ is a unit vector in the x direction, and $\mathbf{F}_i$ is the net force on particle i due to interparticle interactions. $\mathbf{R}_i$ is the stochastic contribution to the particle displacement, which is chosen from a Gaussian distribution of zero mean and with a variance given by

$$\langle \mathbf{R}_i \cdot \mathbf{R}_j \rangle = 6 D_0 \Delta t \delta_{ij} . \tag{6}$$

The shear flow was incorporated into the periodic boundary conditions by using the "sliding brick" method of Lees and Edwards [11]. A noncubic simulation cell was used. This cell was chosen to accommodate a bcc crystal in the preferred alignment for shearing, i.e., with (110) planes in the xz plane and a [111] direction parallel to the x axis. The cell geometry was based on the following three Bravais lattice vectors:

$$\begin{aligned} \mathbf{a} &= a\frac{\sqrt{3}}{2^{2/3}}(-1/3, 0, 2\sqrt{2}/3) \\ \mathbf{b} &= a\frac{\sqrt{3}}{2^{2/3}}(1, 0, 0) \\ \mathbf{c} &= a\frac{\sqrt{3}}{2^{2/3}}(-1/3, -\sqrt{2}/\sqrt{3}, -\sqrt{2}/3) . \end{aligned} \tag{7}$$

Here a is the average distance between nearest neighbors and is given by $a = \rho^{-1/3}$. To relate the system dimensions to the Cartesian axes of shear flow, shear gradient, and vorticity, we use the following notation. As lattice vector $\mathbf{b}$ is aligned with the shear flow, the number of unit cells along this vector is called N_x. The only lattice vector with a component in the gradient direction is $\mathbf{c}$. The number of unit cells in this direction is therefore referred to as N_y. Finally, the system dimensions in the vorticity direction are determined by vector $\mathbf{a}$, leading to the number of unit cells along $\mathbf{a}$ being referred to as N_z. The simulation cell is therefore spanned by vectors $N_z\mathbf{a}$, $N_x\mathbf{b}$, and $N_y\mathbf{c}$. Throughout this paper we refer to cell dimensions by using the triplet (N_x, N_y, N_z).

The interparticle potential appropriate for interactions between charged particles in the presence of screening counterions is the screened Coulomb or Yukawa potential:

$$V(\mathbf{r}) = V_0 \exp(-\kappa|\mathbf{r}|)/|\mathbf{r}| . \tag{8}$$

The net force on a particle, $\mathbf{F}_i$, is found by summing the pairwise interactions between particles i and j for $r_{ij} < r_c (i \neq j)$, where r_c is the cutoff radius chosen [12] such that $\kappa r_c > 8$. An increase in κ, the inverse Debye length, corresponds to an increase in the concentration of salt in the solvent and hence increased screening of particle interactions. We chose a value of κ small enough to

allow an equilibrium bcc crystal structure but not to lead to an interparticle potential so long ranged that significant interaction occurred between image particles. All calculations reported in this paper used $\kappa a = 3.1$.

We have used the following reduced units for length ($r^* = r/a$) and temperature ($T^* = 6k_B T/V_0$). The time unit is related to τ_0, the time required for a particle to diffuse a distance of a. τ_0 is given by $a^2/6D_0$. The reduced time step is $\Delta t^* = \Delta t(\tau_0 T^*)$. A value of $\Delta t^* = 0.03$ is used in all calculations, ensuring that $\Delta t < \tau_0/1000$ over the temperature range studied. All time is reported as the number of reduced time steps. By combining Eq. (7) with the expression of the reduced time step, it can be seen that the mean squared amplitude of the stochastic displacement is proportional to the reduced temperature, i.e.,

$$\langle (R^*)^2 \rangle = T^* \Delta t^* . \tag{9}$$

While the shear rate $\dot{\gamma}$ gives a measure of the magnitude of the applied shear rate, a more meaningful variable is the relative magnitude of convection and diffusion. For this reason we express the magnitude of the shear rate as the Deborah number, defined as $\mathrm{De} = \dot{\gamma}\tau_0$.

The reduced temperature T^* establishes the magnitude of the fluctuating displacements due to collisions between colloidal particles and solvent molecules, modeled here by the stochastic bath. The physical motive for identifying this quantity with temperature is the proportionality between the temperature and the self-diffusion constant established by the Stokes-Einstein relation. In colloidal suspensions, however, temperature will also influence the interparticle potential directly by altering the solvent dielectric constant, the equilibrium of the bound surface charges or, in the case of steric stabilization, the influence of the tethered polymer groups. This quantity, T^*, is thus not expected to translate directly to the actual temperature of a suspension. Instead, the reduced temperature simply provides us with an intensive parameter by which the system may be systematically displaced from the equilibrium melting transition.

IV. RESULTS FOR CRYSTAL NUCLEATION UNDER SHEAR

First, we look at crystallization from a homogeneous suspension in the absence of shear flow. A suspension of 216 particles (at a reduced density of 1.0 and an inverse Debye length of 3.1) was equilibrated at $T^* = 0.04$ and then quenched to $T^* = 0.010$. This final temperature was only 40% of the melting temperature $T^*_{\mathrm{melt}} = 0.0256$ and thus represents a substantially supercooled system. The simulation was then run (with no applied shear) for approximately 2.0×10^5 time steps, by which time it had ordered as indicated by the appearance of additional peaks in the radial distribution function characteristic of a bcc structure. The suspension showed no global crystalline order, however, and we concluded that the final phase was polycrystalline. At slightly smaller supercooling no ordering of any kind was observed for runs up to 5.0×10^5 time steps in duration.

Next, we consider how this process is altered by the imposition of a shear flow. We have examined a range of low shear rates with Deborah numbers between 0.01 and 1.0 for the same system as described above. The times required for ordering from the melt are given in Table I. Reflecting the origin of nucleation in rare structural fluctuations, ordering times are erratic, with systems under equivalent conditions (but different initial conditions) ordering in vastly different times. In Fig. 3 we present the time dependence of the scattering intensity I_{lay} at the Bragg peak for a wave vector aligned along the shear gradient for a run at $\mathrm{De} = 0.05$, in which ordering, eventually, took place. Note the long induction time followed by the rapid growth of order. At $\mathrm{De} = 0.01$ and 0.05, one run out of four ordered in approximately 1.6×10^5 time steps while the other three did not order within 5×10^5 time steps. These data suggest that the nucleation rate, as measured as the number of nuclei per unit volume per unit time, is decreasing with increasing shear rate, as expected from the previous discussion. We saw no nucleation above a shear rate of $\mathrm{De} = 0.07$.

A striking observation is the nature of the crystal phase grown in the sheared suspensions. In dramatic contrast to the growth at zero shear, all the crystals grown in the sheared suspensions consisted in a single aligned crystal. This is in agreement with the observations of Ackerson and Clark [1] on aqueous suspensions of charged particles and our expectations from above concerning the preferential alignment of crystallites. The intriguing feature of this result is that the lowest shear rate we studied, $\mathrm{De} = 0.01$, involves a particle being convected only a distance of 0.44 of the nearest neighbor spacing past its neighbor during the crystallization run. Yet this minute perturbation is sufficient to produce a perfectly aligned single style. This remarkable sensitivity is certainly consistent with the action of the shear on the initial crystallites.

V. RESULTS FOR GROWTH UNDER SHEAR FROM A PLANAR SURFACE

To monitor the rate of crystallization at a planar crystal-liquid surface, the runs were carried out in a cell of dimensions (6,14,6) with a starting configuration of eight layers of perfect crystal oriented with the shear gra-

TABLE I. Ordering times from the melt at $T^* = 0.010$. Note that at low shear rates only a fraction of runs ordered within the 5×10^5 time steps and no ordering was observed for $\mathrm{De} > 0.07$.

Deborah number	Number of runs	Number of runs ordered (within 5×10^5 time steps)	Ordering time (time steps)
0	3	3	$(1.7 \pm 0.27) \times 10^5$
0.01	4	1	1.6×10^5
0.05	4	1	1.6×10^5
0.07	2	1	2.9×10^5
0.1	1	0	
0.2	1	0	
1	1	0	

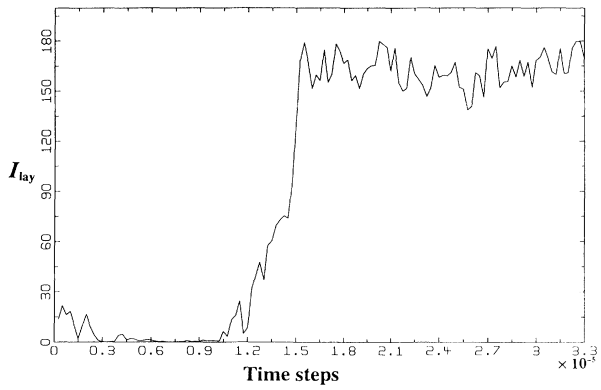

FIG. 3. Time dependence of I_{lay}, the scattered intensity for Bragg scattering from wave vectors aligned with the shear gradient, through the ordering transition at $T^*=0.010$ and De=0.05.

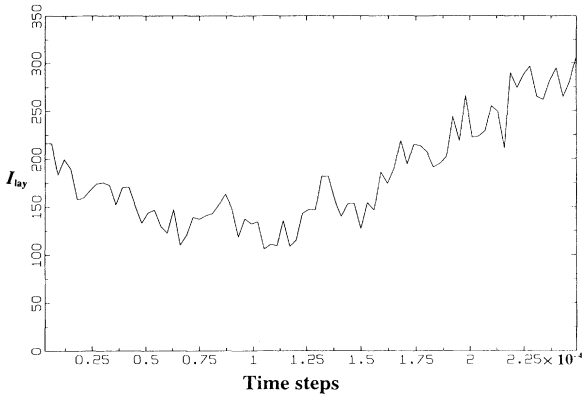

FIG. 5. Time dependence of Bragg scattering aligned with the shear gradient, I_{lay}, for a system at De=0.05 and $T^*=0.021$.

dient normal to the (110) plane and the flow direction parallel to the [111] direction (see Fig. 4). The surfaces of the crystalline slab were (110) planes.

Growth was monitored through the time development of the Bragg peak, as in the previous nucleation study. A typical example of scattering intensity versus time is shown in Fig. 5, this one for growth at $T^*=0.021$ and De=0.05. The large increase in intensity indicates crystallization. The average rate of this increase is reported as the growth rate. (Note that only those runs in which the system ordered are used in this average. As discussed elsewhere [6], the fraction of runs that ordered at a given shear rate is a sensitive function of the shear rate.) The intensity exhibited considerable fluctuations in time. In some runs it stopped midway between the initial condition and complete order for an extended period before continuing to order. A few runs even displayed intense disordering periods during the overall crystallization. There appears to be a region of the T-$\dot{\gamma}$ plane in which steady-state phases of disorder and order both exhibit long-lived stability. We have not observed stable coexistence of the two phases in our small simulated systems.

Many of the runs began with a transient decrease in the Bragg scattering before the increase due to crystallization. This feature appears to result from the rapid relaxation of the perfect crystal structure used in the initial configuration. Finally, we note that there appears to be an induction time before growth commences. This may be an artifact of the unrelaxed initial state. While it is difficult to see how a perfect crystal would impede crystal growth, it is possible that it is the unrelaxed initial crystal-liquid interface that interferes with crystallization.

The growth rates at $T^*=0.021$ are plotted as a function of Deborah number in Fig. 6. They exhibit a distinct minimum at De$\approx$0.05. In the discussion of the preceding section we suggested that the growth rate would be proportional to the effective supercooling. The disordering line in the T-$\dot{\gamma}$ plane for the simulated system is presented in Fig. 7. (This diagram is discussed in detail in Ref. [6].) ΔT_{eff} for $T^*=0.021$, which is the temperature difference between the solid and dashed lines in Fig. 7, exhibits a similar nonmonotonic dependence on De to that shown by the shear rate, including a minimum at De$\approx$0.05. The stabilization of ordered structures in simulations at high shear rates (and hence the origin of the minimum in ΔT_{eff}) has been the subject of some de-

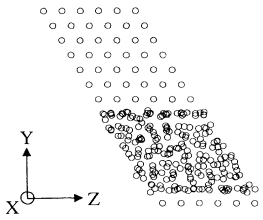

FIG. 4. Projection along the flow direction of a starting configuration consisting of eight bcc (110) layers adjoining an amorphous region.

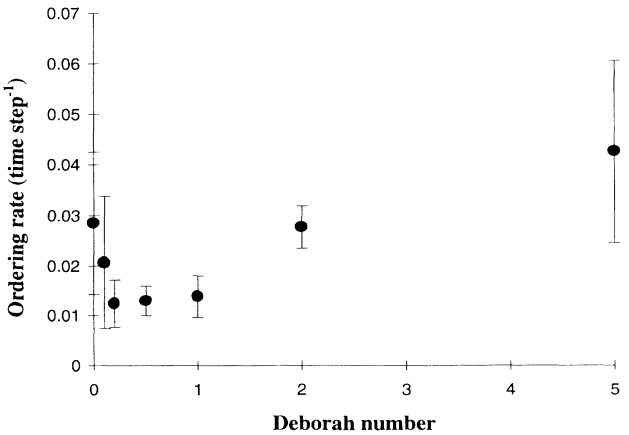

FIG. 6. Ordering rate for ordering from bcc (110) planes vs Deborah number at $T^*=0.021$. The rate of propagation of order is seen to decrease on application of a shear, reaching a minimum at De$\approx$0.5, and then increases with further increases in shear rate.

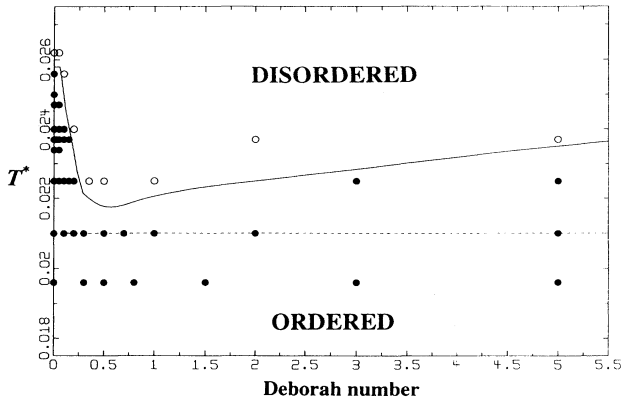

FIG. 7. Nonequilibrium phase diagram over the T^*-De space for systems at $\rho=1$ and $\kappa a=3.1$. Filled circles represent phase points where at least one run using a starting configuration of coexisting order and disorder was observed to order. Open circles represent points where all such runs disordered. The dashed line at $T^*=0.021$ gives the phase cut used when calculating the rates of ordering presented in Fig. 6. The sold line is a line of best fit separating order and disorder. The effective supercooling, ΔT_{eff}, of points along the phase cut at $T^*=0.021$ is the difference in T^* between the solid and dashed lines.

bate [13–15]. Regardless of whether this feature is a computational artifact or not, our results strongly support the proposal that the growth rate (as simulated) and the effective supercooling (as simulated) are strongly correlated.

We can explore this correlation further. Figure 8 plots the rate of ordering at a particular Deborah number against the effective supercooling at that Deborah number. The data appear to divide themselves naturally into two regimes, each characterized by an approximately linear dependence of growth rate on ΔT_{eff}. The dividing line occurs at the Deborah number of De$\approx$0.05, the position of the minima in growth rate (Fig. 6) and effective supercooling (Fig. 7). The filled circles in Fig. 8 represent data taken from the supercooled suspension at low shear rates, i.e., the region characterized by shear-induced disordering. A straight line with a slope of ≈ 58 provides a reasonable fit to these points. For shear rates above the minimum in the effective supercooling (the open circles in Fig. 8), we find that the growth rates versus ΔT_{eff} also lie on a straight line, but with a slope ≈ 19, roughly one third of the value found in the low shear rate regime. We note that the stability of the ordered phase in this high De region must arise from quite different physical origins than at low De. Increasing the shear rate for De>0.05 leads to increased stability of order, i.e., shear-induced *ordering*, as supposed to the shear-induced *disordering* seen for De<0.05. The fact that a linear relationship between growth rate and effective supercooling appears to be a useful representation of the data provides some support for Eq. (4). It also adds weight to the suggestion that pseudoequilibrium ideas, incorporating the effective supercooling, may be useful in explaining the stability of structure in nonequilibrium steady states. We shall return to this point in the following section.

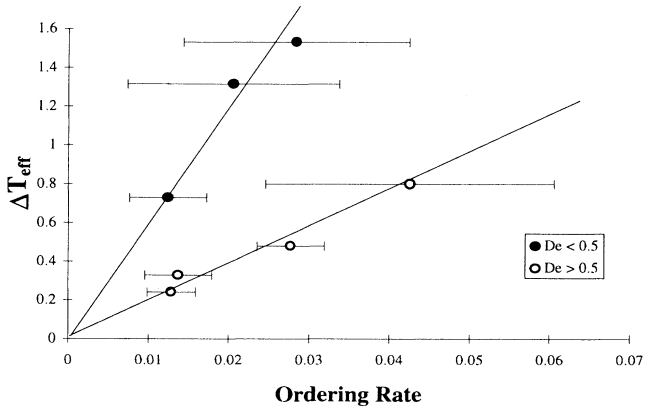

FIG. 8. The ordering rate vs the effective supercooling for a range of De. Open circles are used for rates and supercoolings at De$\geq$0.5 (i.e., for Deborah numbers greater than the minimum in the order-disorder phase boundary in Fig. 7), and closed circles represent points where De<0.5. Lines of best fit are drawn through each set of points.

VI. CONCLUSIONS

In this paper we have presented a preliminary study of crystallization in a dilute charged suspension undergoing shear as simulated by a nonequilibrium Brownian dynamics algorithm. We have observed that nucleation is suppressed by relatively small shear rates. Crystallization did occur at the smallest shear rates we could use, producing a single crystal aligned in the shear flow instead of the polycrystalline order found at zero shear. We note that in real suspensions, crystallization may take place at the walls rather than via homogeneous nucleation. This would expand the range of shear rates over which these shear-aligned crystals can be grown beyond that which we see in simulation.

The major result of the paper is the demonstration that the growth rate of a shearing crystal is approximately proportional to the effective supercooling. The different proportionality constants in the low and high shear rate regimes reflect the very different relationships between the shear flow and order in these two domains under simulation. The qualitative similarity between the dependence of growth rate and supercooling at zero shear and that observed in the shearing suspension between the growth rate and ΔT_{eff} points to some similarities in the underlying nature of the disordering transitions. It would be difficult to reconcile this linear dependence with a model of shear-induced disordering based purely on mechanical disruption. Such a process would depend on the elastic moduli of the crystal, a quantity that does not vanish linearly with the supercooling. On the other hand, we have reported elsewhere [6] the dependence of the position of the order-disorder transition on system size. The only explanation of this dependence to date involves the coupling of the shear flow to long wavelength fluctuations. So we are left, for the moment, with the following picture. These crystallization kinetics studies are

consistent with the stability of the shearing crystal relative to the disordered suspension being described by some sort of "thermodynamic" potential. ("Thermodynamic" is used here in the loose sense that the potential difference between the two phases is a function of only a small set of variables, which includes the effective supercooling.) The observed size dependence, however, requires this "thermodynamic" potential to depend on long wavelength fluctuations in a manner quite different from that found at equilibrium.

This question of the nature of collective stabilization of order away from equilibrium remains an important challenge. Models such as the defect-mediated disordering model [6] provide us with explicit examples of how the enhanced role of long wavelength fluctuations in shearing systems can be incorporated into the familiar formalism of order parameter theories. Recent work by Evans and Baranyai [16] and Peric and Morriss [17] hold out hope of establishing the existence of variational principles that govern steady states far from equilibrium. We believe that experimental and computer simulation studies of kinetics of structural phase transitions under shear will provide a valuable body of data to test and direct the development of these ideas.

ACKNOWLEDGMENT

We gratefully acknowledge generous grants of supercomputer time from the Australian National University Supercomputer Facility and Australian Nuclear Science and Technology Organization.

[1] B. J. Ackerson and N. A. Clark, Phys. Rev. Lett. **46**, 123 (1981); Phys. Rev. A **30**, 906 (1984); Physica **118A**, 221 (1983).
[2] B. J. Ackerson, J. B. Hayter, N. A. Clark, and L. Cotter, J. Chem. Phys. **84**, 2344 (1986).
[3] D. J. Evans, Phys. Rev. A **25**, 2788 (1982).
[4] D. A. Brown and J. Clarke, Phys. Rev. A **34**, 2093 (1986).
[5] M. J. Stevens and M. O. Robbins, Phys. Rev. E **48**, 3778 (1993).
[6] S. Butler and P. Harrowell, J. Chem. Phys. **103**, 4653 (1995).
[7] B. J. Ackerson and P. N. Pusey, Phys. Rev. Lett. **61**, 1033 (1988); B. J. Ackerson, J. Phys. Condens. Matter **2**, SA389 (1990).
[8] W. Xue and G. S. Grest, Phys. Rev. A **40**, 1709 (1989); W. Xue and G. S. Grest, Phys. Rev. Lett. **64**, 419 (1990).
[9] Y. Monovoukas and A. P. Gast, J. Colloid Interface Sci. **128**, 533 (1989).
[10] D. L. Ermak and J. A. McCammon, J. Chem. Phys. **69**, 1352 (1978).
[11] Q. W. Lees and S. F. Edwards, J. Phys. C **5**, 1921 (1972).
[12] M. O. Robbins, K. Kremer, and G. S. Grest, J. Chem. Phys. **88**, 3286 (1988).
[13] D. J. Evans and G. P. Morriss, Phys. Rev. Lett. **56**, 2172 (1986).
[14] W. Loose and S. Hess, Rheol. Acta **28**, 91 (1989).
[15] W. Loose and G. Ciccotti, Phys. Rev. A **45**, 3859 (1992).
[16] D. J. Evans and A. Baranyai, Phys. Rev. Lett. **67**, 2597 (1991).
[17] M. Peric and G. P. Morriss, Mol. Phys. **84**, 1049 (1995).

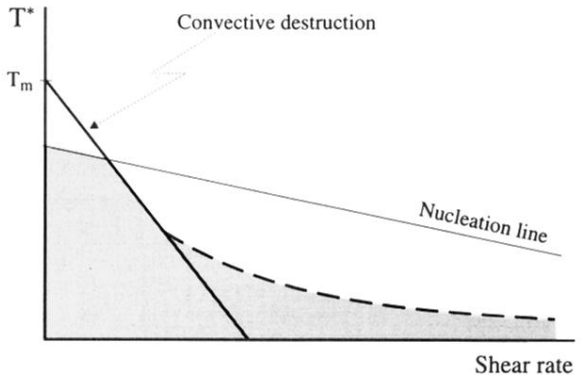

FIG. 1. Schematic representation of nucleation behavior under variations in temperature and shear rate. The "nucleation line" shows the expected decrease in nucleation due to destabilization of the equilibrium structure by the applied shear. This line is cut by the line representing the effect of "convective destruction" of nuclei. At low temperatures, where nucleation occurs at many sites, a nonlinearity is expected in the convective destruction of nuclei. This is represented by the dashed line. The shaded area is therefore the window of temperatures and shear rates within which nucleation and growth of order are expected to occur.

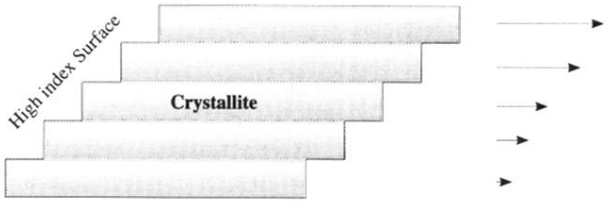

FIG. 2. Schematic diagram showing a crystallite undergoing plane-over-plane sliding under shear. The result of layers sliding over one another is the production of stepped high index surfaces from which growth must occur if the cluster is not to be destroyed by convection.